Talanta 85 (2011) 1260–1264

Contents lists available at ScienceDirect

Talanta

journal homepage: www.elsevier.com/locate/talanta

Enzyme-free amperometric sensing of hydrogen peroxide and glucose at a hierarchical Cu_2O modified electrode

Song Li, Yajie Zheng, Gaowu W. Qin*, Yuping Ren, Wenli Pei, Liang Zuo

Key Laboratory for Anisotropy and Texture of Materials (MoE), Northeastern University, Shenyang 110819, China

ARTICLE INFO

Article history:
Received 30 December 2010
Received in revised form 10 May 2011
Accepted 19 May 2011
Available online 26 May 2011

Keywords:
Amperometric sensing
Hierarchical structure
Hydrogen peroxide
Glucose

ABSTRACT

In this paper, an enzyme-free amperometric electrochemical sensor was fabricated by casting Nafion-impregnated Cu_2O particles onto a glassy carbon electrode. A dual dependence of peak current on sweeping rate, which can be attributed for the accumulation of reaction products, was observed on the sensor. Electrochemical analysis of the particulate Cu_2O for detecting H_2O_2 and glucose is described, showing remarkable sensitivity in both cases. The estimated detection limits and sensitivities for H_2O_2 (0.0039 μM, 52.3 mA mM^{-1} cm^{-2}) and glucose (47.2 μM, 0.19 mA mM^{-1} cm^{-2}) suggest that the response for H_2O_2 detection was much higher than for glucose detection. Electron microscopy observation suggested that the hierarchical structures of Cu_2O resulting from self-assembly of nanocrystals are responsible for the specific electrochemical properties.

1. Introduction

Detecting hydrogen peroxide and glucose levels in foods and blood by electrochemical method with a modified electrode has been receiving much attention for many years from chemical, clinical and environmental communities [1–4]. Since the pioneering work by Clark on the enzymatic electrode for determination of glucose level in blood, various enzymatic sensing techniques have been proposed and successfully developed. Despite positive attributes of enzymatic biosensors, the main drawbacks associated with their applications are the insufficient stability originated from the nature of the enzymes and the complexity of enzyme immobilization process, regardless of the employment of artificial mediator or direct electron transfer [5]. Therefore, a growing interest in the development of new-generation electrode without using enzyme for detecting hydrogen peroxide or glucose has been aroused in this field.

To meet the demands of enzymeless sensing, modifying kinds of electrodes by numerous nanostructured materials has been intensively investigated. For instance, to detect glucose, nanoporous and nanotubular Pt [6,7], Ni [8], carbon nanotubes [9], metal oxides [10], and their hybrids [11–13] have been applied to construct modified electrode. Cuprous oxide (Cu_2O), as an important p-type semiconductor, demonstrates potential applications in the fields of sensing and solar energy conversion due to its proper redox potentials and excellent stability in air and solutions. The synthesis of a variety of Cu_2O nanostructures has been reported, including hollow structures [14–16], nanotubes/nanowires [17], and nanocubes [18]. For electrochemical sensing applications, substrate adsorption on electrode surface and prompt charge transfer play essential roles. Control over the morphology of electrode nanomaterial is therefore extremely important [10]. In this work, hierarchical nanocrystals of Cu_2O were used to construct an enzyme-free electrode for detecting hydrogen peroxide and glucose. The results showed that a high electrochemical performance was provided by the unique structure.

2. Experimental

The Cu_2O nanoparticles were synthesized by a low temperature chemical method, which was similar to literature [16,19]. In a typical procedure, 0.225 g PVP (polyvinyl pyrrolidone, K30) and 0.400 g Cu $(CH_3COO)_2{\cdot}H_2O$ were dissolved in sequence in 25 ml DMF (N,N-dimethylformamide) at room temperature under stirring. Then 0.100 g $NaBH_4$ was added to the solution and stirring was remained for several minutes until the additives dissolved in the DMF solvent. Then the resultant transparent solution was transferred to a 75 °C water bath and was maintained for 20 min. The modified electrode was prepared as follows. 10 mg of the final Cu_2O particles, after washing, was dispersed in 2 ml Nafion solution (0.1%, Sigma–Aldrich). 2.5 μl of the suspension with dispersed Cu_2O was cast on pre-treated ϕ 3 mm glassy carbon electrode (denoted as Cu_2O/Nafion/GCE). Before modification, the bare GCE was polished to a mirror-like surface with 0.3 and 0.05 μm alumina slurry, and then washed ultrasonically in deionized water, 50% (v/v) HNO_3 solution, ethanol, and water for a few minutes.

* Corresponding author. Tel.: +86 24 83683772; fax: +86 24 83686455.
E-mail address: qingw@smm.neu.edu.cn (G.W. Qin).

0039-9140/$ – see front matter © 2011 Elsevier B.V. All rights reserved.
doi:10.1016/j.talanta.2011.05.033

Electrochemical measurements were carried out on a Zahner IM6 electrochemical analyzer with a conventional three-electrode cell. The as-fabricated Cu_2O/Nafion/GCE was used as the working electrode with a platinum foil as an auxiliary electrode and a KCl saturated Ag/AgCl reference electrode. The measurements were performed in aqueous phosphate buffer solution (PBS: 0.1 M, pH 7.4). X-ray diffraction (XRD) pattern of the obtained Cu_2O nanospheres was collected on an X'Pert PRO diffractometer (Panalytical) with Cu Kα irradiation. Scanning electron microscopy (SEM) and transmission electron microscopy (TEM) images were obtained by employing a JEOL JEM-7100F microscope and a JEOL 2100F microscope.

3. Results and discussion

The morphology of the Cu_2O nanoparticles prepared at 75 °C is displayed in Fig. 1a, which shows that the product is composed of uniform nanospheres with an average size of 200 nm and a very narrow size distribution. TEM image (Fig. 1b) reveals that the Cu_2O nanospheres are the results of self-assembly of smaller Cu_2O nanocrystals. It is worthy of note that, by assembling nanocrystals into a hierarchical structure, the agglomeration of the nanospheres could be prevented [20]. BET specific surface area via nitrogen sorption analysis (Fig. 2a) of the as-synthesized Cu_2O is 13.1 $m^2\ g^{-1}$. Such features of high surface area-to-volume ratio as well as the compact assembling of nanocrystals into polycrystalline spheres provide a very large number of interaction sites for electrochemical reactions and good conductivity [21,22]. Furthermore, as we reported on enhancing the catalytic activity of Pt nanomaterials by linearly assembly of Pt nanoparticles into nanowires [23], grain boundaries are expected to be very helpful for improving the electrochemical performance of the Cu_2O nanospheres. The selected area electron diffraction (SAED) ring pattern that corresponds to a small number of nanospheres can be indexed to cubic Cu_2O. Further crystallinity and phase information for the product were provided by the X-ray diffraction (XRD) pattern. As shown in Fig. 2, all the diffraction peaks in the pattern match well with the cubic crystal structure of the Cu_2O phase (space group: *Pn3m*, ICDD No. 77-0199). The narrow and sharp peaks in the pattern indicate that the Cu_2O nanospheres are highly crystallized, which could have positive effects for the electron transfer in electrochemical reactions.

The electrochemical properties of the electrodes are often characterized by cyclic voltammetry (CV). Fig. 3 shows CV response of

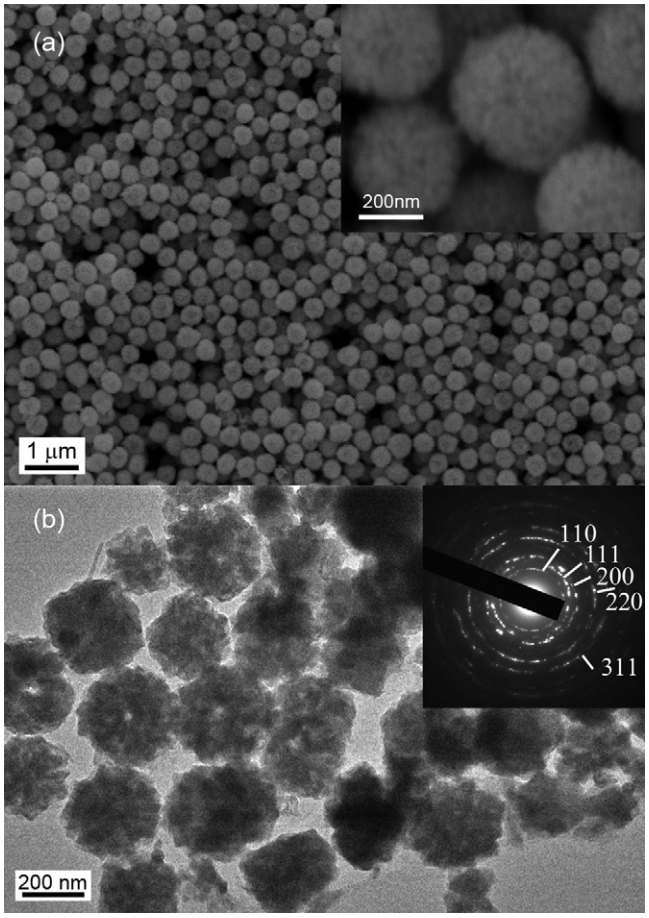

Fig. 1. SEM (a) and TEM (b) morphological images of as-synthesized Cu_2O nanocrystals. Inset of (a) is a magnified SEM image. Inset of (b): electron diffraction patterns taken from some Cu_2O nanospheres. The rings match well with cubic Cu_2O structure.

Cu_2O/Nafion/GC electrode in pH 7.4 PBS at sweeping rate between 25 mV s^{-1} and 1000 mV s^{-1}. The cathodic and anodic peak currents can be ascribed to electrochemical reactions of Cu_2O, including CuO/Cu_2O redox couple and reactions of the produced CuO layer [24].

Fig. 4 The increase of cathodic and anodic peak currents (i_{pc} and i_{pa}), as well as small shifts of the cathodic and anodic peak

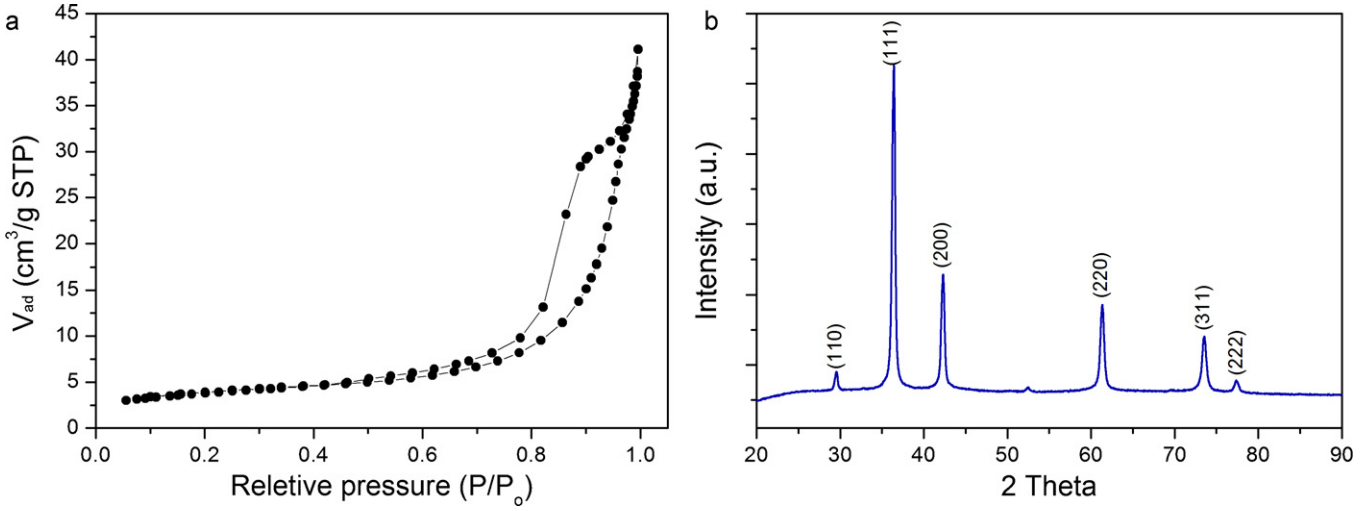

Fig. 2. (a) Nitrogen adsorption–desorption isothermal curve of the as-synthesized Cu_2O nanoparticles. (b) XRD pattern of Cu_2O nanoparticles synthesized at 75 °C for 20 min. All diffraction peaks can be indexed to Cu_2O (ICDD No. 77-0199).

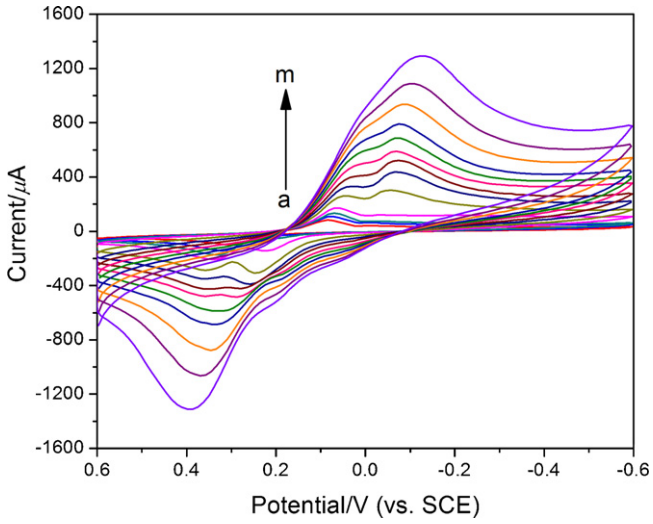

Fig. 3. Cyclic voltammograms of a Cu_2O/Nafion/GC electrode in 0.10 M PBS (pH 7.4) by sweeping at different scan rates. The scan rates from inner to outer are: 0.025, 0.05, 0.075, 0.1, 0.2, 0.3, 0.4, 0.5, 0.6, 0.7, 0.8, 0.9, 1.0 V s^{-1}, respectively.

potentials could be observed with the increase of the scan rate. Fig. 4 shows the dependence of peak current i on scan rate v which can be described by the equation $i = Av^k$, where A is a material-related constant. The parameter k is expected to take a value 0.5 and 1.0 for diffusion-controlled and adsorption-controlled reactions, respectively [3,12,25]. At lower scan rates ($v < 0.60$ V s^{-1}), a linear response of peak current on square root of the scan rate was observed, indicating that the electron transfer of Cu_2O/Nafion complex with the GC electrode was a diffusion-controlled process. At higher scan rates ($v > 0.6$ V s^{-1}), the current peaks increased linearly with the scan rate, suggesting that the electron transfer reaction was controlled by surface adsorption [26]. The switch of a diffusion-controlled behavior to a diffusionless one is because there is not sufficient time for the reaction species to diffuse across the Cu_2O/Nfs layers at higher scan rates. Therefore, the reaction products may accumulate on the surface of the electrode. Similar phenomena have been observed on electrocatalytic detection of dopamine on silanized graphene modified GC electrode [27].

Fig. 5a shows the amperometric response of the Cu_2O/Nf modified electrode in pH 7.4 PBS upon addition of H_2O_2 in a 1 μM

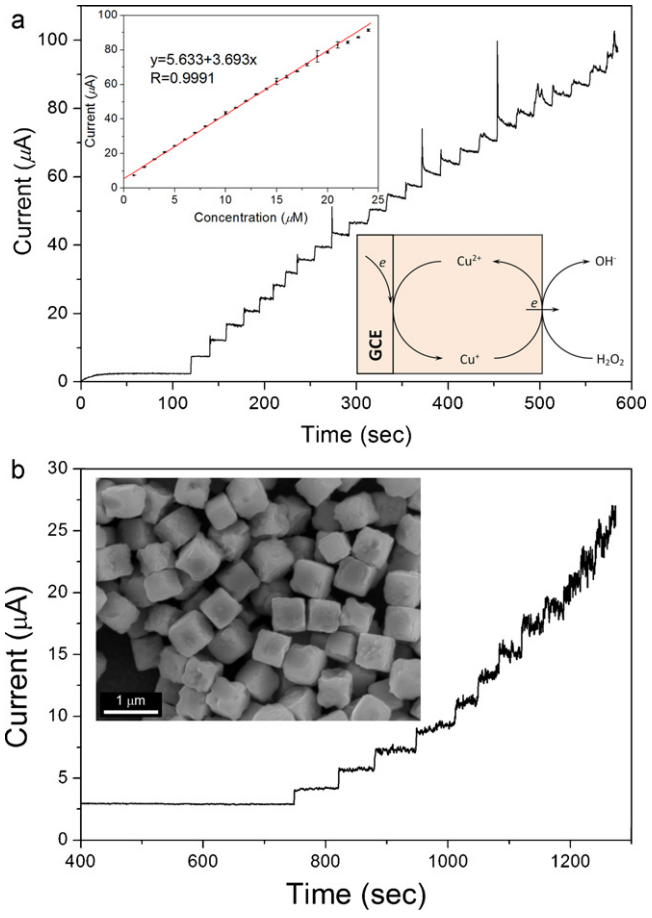

Fig. 5. (a) Amperometric response of Cu_2O/NFs/CG electrode with successive addition of 1 μM H_2O_2 to 0.1 M PBS (pH 7.4) at −0.2 V. The insets show the calibration plot and schematic mechanism of reduction of H_2O_2 on surface of Cu_2O/NFs/CG electrode. (b) The SEM image of the Cu_2O cubes synthesized from Benedict's solution and their current-time response under the same conditions as in (a).

step at −0.2 V. The response time for detecting H_2O_2 to obtain a steady current was less than 0.5 s. The calibration curve in the inset shows a highly linear relationship (ca. $R^2 = 0.9991$) between the current and concentration of H_2O_2 in a broad range below 22 μM, and features a detection sensitivity of a 3.693 μA μM^{-1}. Calculated

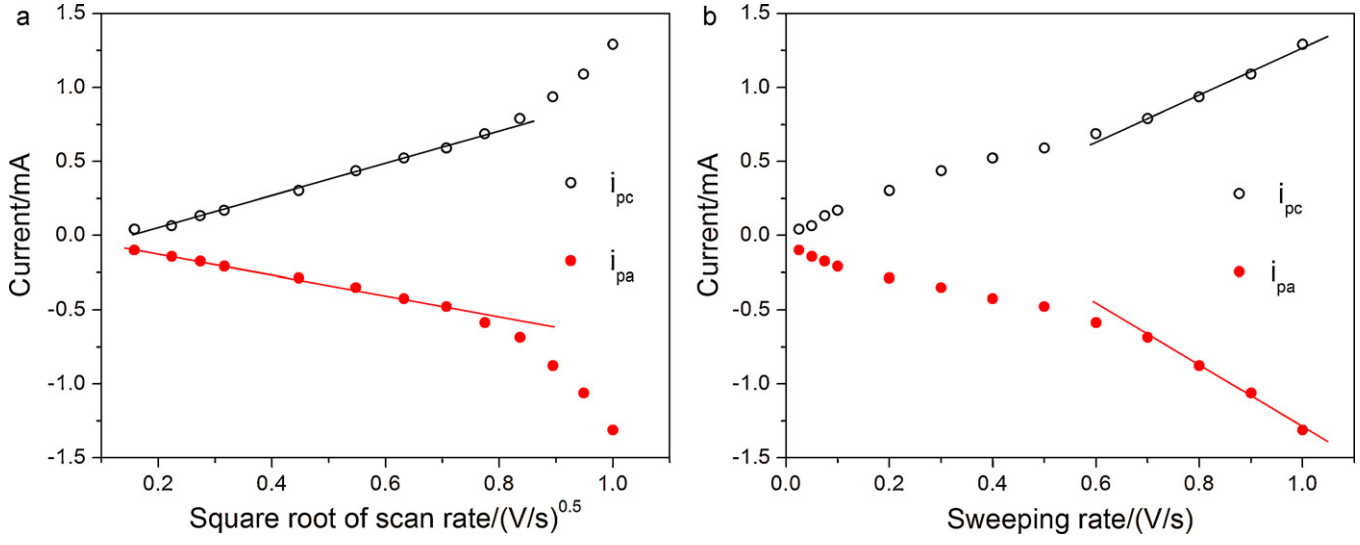

Fig. 4. Peak current as a function of (a) square root of scan rate and (b) scan rate.

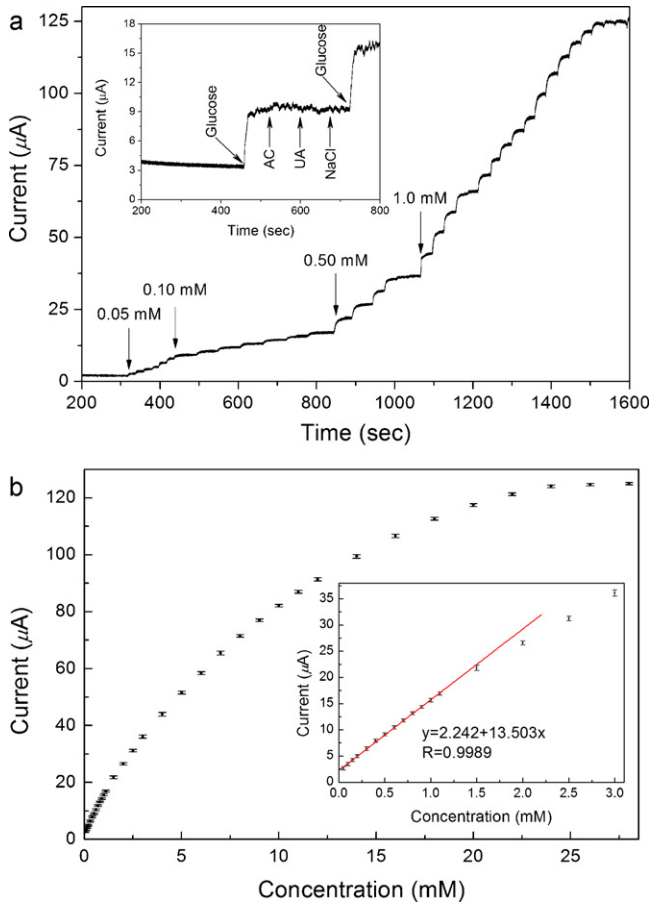

Fig. 6. (a) Amperometric response of the Cu_2O/NFs/GC electrode with successive addition of glucose in a 0.1 M NaOH solution at 0.5 V. Inset of (a) shows the anti-interference property of the modified electrode. (b) Dependence of steady current of the modified electrode on concentration of glucose. The linear part of the calibration curve was shown in the inset of (b).

detection limit was 0.39×10^{-7} mol L^{-1} by $3s/\sigma$, where s and σ are standard deviation of the background current and slope of the calibration curve respectively. The detection limit is much lower than those reported electrode modified by other materials [9,28,29]. As schematically shown in inset of Fig. 5a, the electrochemical detection of H_2O_2 reduction is assisted by Cu^+/Cu^{2+} redox couple. In the viewpoint of electrocatalysis, effective adsorption of the reactants on the electrode/electrolyte interface and fast charge transportation in the electrode are crucial [13]. In this work, not only the specific surface area and charge-transport channels gets enhanced due to the hierarchical structure of Cu_2O as a result of self-assembly of nanocrystals, but also many grain boundaries with high electrocatalytic performance are provided by the compact attachment of the comprising nanocrystals. To further demonstrate the merit of the hierarchical structure, cubic shaped Cu_2O with smooth surface (Fig. 5b) were synthesized via reduction of Benedict's solution [30], and Fig. 5b shows their current-time response towards H_2O_2 under the same experimental condition, including electrolyte, potential, temperature, and amount the successive H_2O_2 additives. It was found that the electrode modified with the above Cu_2O cubes exhibited a steady response at low concentrations of H_2O_2. However, the response cannot remain steady after the concentration of H_2O_2 exceeds 7 μM, demonstrating their narrow working range. The deterioration of electrocatalytic property is believed resulting from morphology change.

The chronaoamperometric current responses of the prepared Cu_2O/Nfs/GC electrode to glucose were measured in 0.10 M NaOH solution under continuous stirring. Fig. 6a shows a typical response of the electrode to the successive addition of glucose at a working potential of 0.5 vs. Ag/AgCl. The response of the electrode to glucose is rapid and a steady state current signal can be reached within 4 s upon addition of the glucose solution. The corresponding calibration curve for glucose concentration is illustrated in Fig. 6b, which shows a linear relationship range from 0.05 mM to 1.1 mM. The fitting equation is $I(\mu A) = 2.242 + 13.503c$ (mM) with a correlation coefficient of 0.9989. The detection limit was estimated as 47.2 μM at a signal/noise ratio of 3. Anti-interference effect of the modified electrode was tested by adding 0.2 mM glucose, followed with additions of 0.01 mM ascorbic acid (AC), 0.04 mM uric acid (UC) and 0.04 mM NaCl in 0.1 M NaOH solution. The responses shown in inset of Fig. 6a demonstrate that the interference effect from small amount of AC, UC and NaCl can be neglected.

4. Conclusion

In summary, spherical Cu_2O nanoparticles comprising smaller nanocrystals were synthesized in a simple chemical way. By coating Cu_2O/NFs onto GCE surface, enzyme-free sensors were constructed for detecting hydrogen peroxide and glucose. The modified electrodes showed fast amperometric response and high sensitivity. This is because of the increased electroactive surface area and compact attachment of Cu_2O nanocrystals resulting from the hierarchical structures. The detection limits for H_2O_2 and glucose are 0.0039 μM and 47.2 μM, respectively. These properties are believed to be very helpful for developing new biosensors and biodevices without enzyme.

Acknowledgments

This work was supported by NSFC (grant no. 51002026) and the Fundamental Research Funds for the Central Universities (grant no. N090302002 and N100702001). The corresponding author acknowledges Program for New Century Excellent Talents in University (no. NCET-09-0272) and Liaoning Program for Excellent Talents in University (no. 2009R23).

References

[1] S. Hrapovic, Y. Liu, K.B. Male, J.H.T. Luong, Anal. Chem. 76 (2004) 1083–1088.
[2] J. Wang, M. Musameh, Y. Lin, J. Am. Chem. Soc. 125 (2003) 2408–2409.
[3] L. Li, Z. Du, S. Liu, Q. Hao, Y. Wang, Q. Li, et al., Talanta 82 (2010) 1637–1641.
[4] W. Lu, F. Liao, Y. Luo, G. Chang, X. Sun, Electrochim. Acta 56 (2011) 2295–2298.
[5] S. Park, H. Boo, T.D. Chung, Anal. Chim. Acta 556 (2006) 46–57.
[6] S. Park, T.D. Chung, H.C. Kim, Anal. Chem. 75 (2003) 3046–3049.
[7] J.H. Yuan, K. Wang, X.H. Xia, Adv. Funct. Mater. 15 (2005) 803–809.
[8] K.E. Toghill, L. Xiao, M.A. Phillips, R.G. Compton, Sens. Actuators B: Chem. 147 (2010) 642–652.
[9] F. Gao, J. Yin, Z. Yao, M. Li, L. Wang, J. Electrochem. Soc. 157 (2010) F35–F39.
[10] T. Kong, Y. Chen, Y. Ye, K. Zhang, Z. Wang, X. Wang, Sens. Actuators B: Chem. 138 (2009) 344–350.
[11] D. Rathod, C. Dickinson, D. Egan, E. Dempsey, Sens. Actuators B: Chem. 143 (2010) 547–554.
[12] L.-C. Jiang, W.-D. Zhang, Biosens. Bioelectron. 25 (2010) 1402–1407.
[13] W. Wang, Z. Li, W. Zheng, J. Yang, H. Zhang, C. Wang, Electrochem. Commnun. 11 (2009) 1811–1814.
[14] H. Zhang, D. Zhou, L. Zhang, D.-F. Zhang, L. Guo, L. He, et al., J. Nanosci. Nanotechnol. 9 (2009) 1321–1325.
[15] L. Xu, J. -jie Zhu, Sci. Adv. Mater. 1 (2009) 121–124.
[16] Y. Chang, J.J. Teo, H.C. Zeng, Langmuir 21 (2005) 1074–1079.
[17] D.P. Singh, N. Ali, Sci. Adv. Mater. 2 (2010) 295–335.
[18] L. Gou, C.J. Murphy, J. Mater. Chem. 14 (2004) 735–738.
[19] J. Zhang, J. Liu, Q. Peng, X. Wang, Y. Li, Chem. Mater. 18 (2006) 867–871.
[20] W. Lu, S. Gao, J. Wang, J. Phys. Chem. C. 112 (2008) 16792–16800.
[21] M. Willander, L.L. Yang, A. Wadeasa, S.U. Ali, M.H. Asif, Q.X. Zhao, et al., J. Mater. Chem. 19 (2009) 1006–1018.
[22] Y. Li, H.J. Schluesener, S. Xu, Gold Bull. 43 (2010) 29–41.
[23] G.W. Qin, W. Pei, X. Ma, X. Xu, Y. Ren, W. Sun, et al., J. Phys. Chem. C. 114 (2010) 6909–6913.
[24] L. Zhang, Y. Ni, H. Li, Microchim. Acta 171 (2010) 103–108.

[25] N.F. Atta, A. Galal, F.M. Abu-Attia, S.M. Azab, J. Electrochem. Soc. 157 (2010) F116–F123.
[26] W. Zheng, J. Li, Y.F. Zheng, Biosens. Bioelectron. 23 (2008) 1562–1566.
[27] S. Hou, M.L. Kasner, S. Su, K. Patel, R. Cuellari, J. Phys. Chem. C. 114 (2010) 14915–14921.
[28] X. Zhang, G. Wang, W. Zhang, N. Hu, H. Wu, B. Fang, J. Phys. Chem. C. 112 (2008) 8856–8862.
[29] H.L. Zhang, Y. Ni, J. Li, K. Liao, G. Zhao, Electrochem. Commnun. 11 (2009) 812–815.
[30] Y. Cao, J. Fan, L. Bai, F. Yuan, Y. Chen, Cryst. Growth Des. 10 (2010) 232–236.